Journal of the American College of Cardiology
© 2010 by the American College of Cardiology Foundation
Published by Elsevier Inc.

Vol. 56, No. 18, 2010
ISSN 0735-1097/$36.00
doi:10.1016/j.jacc.2010.05.045

Cardiac Genetics

Nebulette Mutations Are Associated With Dilated Cardiomyopathy and Endocardial Fibroelastosis

Enkhsaikhan Purevjav, MD, PhD,* Jaquelin Varela, BS,† Micaela Morgado, MS,† Debra L. Kearney, MD,‡ Hua Li, PhD,† Michael D. Taylor, MD, PhD,† Takuro Arimura, DVM, PhD,‖ Carole L. Moncman, PhD,¶ William McKenna, MD,# Ross T. Murphy, MD,# Siegfried Labeit, MD,** Matteo Vatta, PhD,† Neil E. Bowles, PhD,†† Akinori Kimura, MD, PhD,‖ Aladin M. Boriek, PhD,§ Jeffrey A. Towbin, MD*

Cincinnati, Ohio; Houston, Texas; Tokyo, Japan; Lexington, Kentucky; London, United Kingdom; Mannheim, Germany; and Salt Lake City, Utah

Objectives Four variants (K60N, Q128R, G202R, and A592E) in the nebulette gene were identified in patients with dilated cardiomyopathy (DCM) and endocardial fibroelastosis. We sought to determine if these mutations are cardiomyopathy causing.

Background Nebulette aligns thin filaments and connects them with the myocardial Z-disk, playing a role in mechanosensation.

Methods We generated transgenic mice with cardiac-restricted overexpression of human wild-type or mutant nebulette. Chimera and transgenic mice were examined at 4, 6, and 12 months of age by echocardiography and cardiac magnetic resonance imaging. The hearts from embryos and adult mice were assessed by histopathologic, immunohistochemical, ultrastructural, and protein analyses. Rat H9C2 cardiomyoblasts with transient expression of nebulette underwent cyclic mechanical strain.

Results We identified lethal cardiac structural abnormalities in mutant embryonic hearts (K60N and Q128R). Founders of the mutant mouse lines developed DCM with severe heart failure. An irregular localization pattern for nebulette and impaired desmin expression were noted in the proband and chimeric Q128R mice. Mutant G202R and A592E mice exhibited left ventricular dilation and impaired function with specific changes in I-band and Z-disk proteins by 6 months of age. The mutations modulated distribution of nebulette in the sarcomere and Z-disk during stretch of H9C2 cells.

Conclusions Nebulette is a new susceptibility gene for endocardial fibroelastosis and DCM. Different mutations in nebulette trigger specific mechanisms, converging to a common pathological cascade leading to endocardial fibroelastosis and DCM. (J Am Coll Cardiol 2010;56:1493–502) © 2010 by the American College of Cardiology Foundation

Dilated cardiomyopathy (DCM), characterized by left ventricular (LV) dilation and dysfunction, is believed to be of genetic origin in approximately 35% or more of all cases (1). Endocardial fibroelastosis (EFE), associated with diffuse LV endocardial thickening due to proliferation of fibrous and elastic tissue, is a rare cardiac disorder with poor prognosis that occurs in infants and young children (2). Although virus-induced fetal myocarditis or X-linked Barth or autosomal recessive inherited genes have been reported to be causative for EFE, most cases are of unknown etiology (3). Various molecular mechanisms are involved in the

See page 1503

From *The Heart Institute, Cincinnati Children's Hospital Medical Center, Cincinnati, Ohio; †Section of Cardiology, Department of Pediatrics, Baylor College of Medicine, Houston, Texas; ‡Section of Pathology, Department of Pediatrics, Baylor College of Medicine, Houston, Texas; §Department of Medicine, Baylor College of Medicine, Houston, Texas; ‖Department of Molecular Pathogenesis, Medical Research Institute and Laboratory of Genome Diversity, School of Biomedical Science, Tokyo Medical and Dental University, Tokyo, Japan; ¶Department of Molecular and Cellular Biochemistry, University of Kentucky, Lexington, Kentucky; #Department of Cardiology, The Heart Hospital, London, United Kingdom; **Department of Integrative Pathophysiology, University of Medicine, Mannheim, Germany; and the ††Department of Pediatrics, University of Utah, Salt Lake City, Utah. This work was supported by Postdoctoral Fellowship and Beginning-Grant-in-Aid (Drs. Purevjav and Towbin) and Scientist Development (Dr. Bowles) grants from the American Heart Association. Dr. Towbin was supported by the Children's Cardiomyopathy Foundation and by the National Institutes of Health, National Heart, Lung, and Blood Institute (PCMR and PCSR RO1 HL0870000-01A1). All other authors have reported that they have no relationships to disclose.

Manuscript received December 10, 2009; revised manuscript received April 21, 2010, accepted May 18, 2010.

JACC Vol. 56, No. 18, 2010
October 26, 2010:1493–502

Abbreviations and Acronyms

α-MyHC = α-myosin heavy chain
cDNA = clone deoxyribonucleic acid
DCM = dilated cardiomyopathy
EFE = endocardial fibroelastosis
LV = left ventricular
RI = relative intensity
Tg = transgenic
WT = wild type

development of these disorders because of the overlapping functions of cytoskeletal proteins, beginning from their involvement in sarcomeric structure, to their functions in cardiac differentiation, myofibrillogenesis, and transcriptional regulation (4,5).

The nebulin family is a group of actin-binding proteins whose universal feature is the presence of "nebulin-repeats" that bind a single actin subunit and is involved in tropomyosin-troponin assembly (6). Moreover, expression of specific nebulin isoforms with specific numbers of "nebulin repeats" correlates thin filament length in a striated muscle-specific manner (7). The only cardiac-specific member, nebulette *(NEBL)*, a 107 kDa protein appears to be involved in early myogenesis and myofibrillar organization in cardiomyocytes (8,9). The nebulin-repeat domain of nebulette tethers it to the I-band, while the C-terminus is embedded inside the Z-lines, interacting with α-actinin2 (9), the titin-PEVK (7), myopalladin (10), desmin (11), and filamin C (12). Additionally, nebulette significantly increases the affinity of tropomyosin-troponin for F-actin (13). Involvement in these key protein-protein interactions suggests the functional importance of nebulette in the heart.

Nebulette polymorphism (Asn654Lys) in the actin-binding motif has been previously associated with non-familial DCM (14). To determine whether *NEBL* plays roles in the genetic and cellular basis of cardiomyopathies, we screened *NEBL* in patients with DCM. Transgenic (Tg) mice with cardiac-specific overexpression of *NEBL* were created, and functional analysis was pursued to explore the molecular mechanisms responsible for the development and regulation of the clinical phenotypes seen in humans. We investigated the effect of the mutations under mechanical stretch by applying cyclic mechanical strain in transient nebulette-expressing H9C2 cardiomyoblasts.

Methods

Mutational analysis. We assessed genomic deoxyribonucleic acid (DNA) from 260 patients with DCM recruited after informed consent using direct sequencing methods (ABI 3730). Cytoskeletal and sarcomeric genes were investigated for mutations as previously described (15). For each variant identified, available family members and 300 unrelated ethnic-matched persons were screened.

Human heart immunohistochemistry. A paraffin-embedded sample of the explanted heart from patient S84-5162 carrying the Q128R *NEBL* variant was available for analysis after informed consent. As a control, heart tissue was obtained from a normal donor subject (head trauma victim)

A

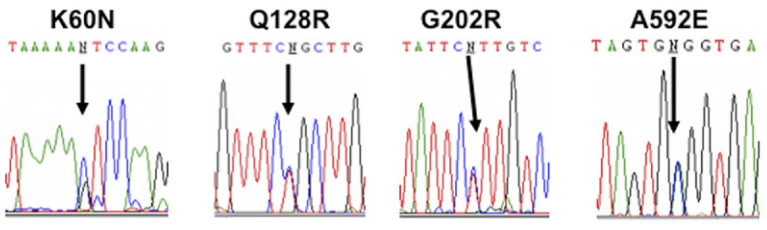

B

ID	Mutation	Localization	Gender	Age at onset (yr)	Clinical diagnosis	FH	NYHA	LVEDD (mm)	%FS
H424214	K60N	Actin-binding domain	M	55 y	DCM	No	II	84	23
S84-516 2	Q128R	Actin-binding domain	F	NB	DCM+EFE	N/A	II	N/A	10
H693839	G202R	Nebulin repeats (I band)	F	41	DCM	No	II	65	18
73-2	A592E+ M374V in α-actinin2	Nebulin repeats (Z-disk)	F	NB	DCM	No	I	N/A	20

Figure 1 Nebulette Mutations in Cardiomyopathy

(A) Sequence electropherograms of *NEBL* showing the disease-associated nucleotide substitutions. **(B)** Genetic and clinical features of patients carrying *NEBL* mutations. DCM = dilated cardiomyopathy; EFE = endocardial fibroelastosis; FH = family history; LVEDD = left ventricular end-diastolic dimension; NB = newborn; NYHA = New York Heart Association; %FS = percent fractional shortening.

after informed consent of the victim's family. The samples were dewaxed and stained with nebulette, desmin, myopalladin, and α-actinin2 antibodies using standard techniques (15).

Generation and characterization of α-MyHC-nebulette transgenic embryos and mice. Full-length 3.1 kb human nebulette wild-type (WT) clone DNA (cDNA [NM-006393]) was amplified by reverse transcription–polymerase chain reaction from human heart ribonucleic acid (Ambion, Houston, Texas) and ligated into vector containing the murine α-myosin heavy chain (α-MyHC) promoter and downstream human growth hormone gene (Dr. Jeffrey Robbins, Cincinnati Children's Hospital Medical Center, Cincinnati, Ohio). Mutants (K60N, Q128R, G202R, and A592E) were created using the QuikChange Site-directed mutagenesis kits (Stratagene, La Jolla, California). The transgenic (Tg) mice were created according to the Baylor College of Medicine animal regulations. Offspring were genotyped using polymerase chain reaction of genomic DNA. Transcription and protein expression levels were confirmed by real-time quantitative reverse transcription–polymerase chain reaction and Western blotting. Embryos were studied at E7.5, 9.5, 12.5, and 16.5 stages (n >3).

To determine latent exercise intolerance, Tg and age- and sex-matched non-Tg mice underwent graded treadmill testing at 4 and 6 months of age (n ≥5). The treadmill (Exer-6M, Columbus Instruments, Columbus, Ohio) was set at a slope of 15° with a starting speed of 16 m/min; the speed was increased by 2 m/min every 5 min until the mouse exhibited signs of exhaustion, and total running distance was recorded. Echocardiography and cardiac magnetic resonance imaging was performed (n = 5) as described previously (15).

Assessment of transgenic mouse hearts. Mouse hearts were studied by histology, immunohistochemistry, Masson trichrome, or transmission electron microscope, as described previously (15). Antibodies against nebulette and myopalladin (11), α-actinin2 (Upstate [Millipore], Billerica, Massachusetts), desmin (Abcam, Cambridge, Massachusetts), Z-band alternatively spliced PDZ-motif protein (ZASP; Dr. Georgine Faulkner, ICGEB, Trieste, Italy), tropomy-

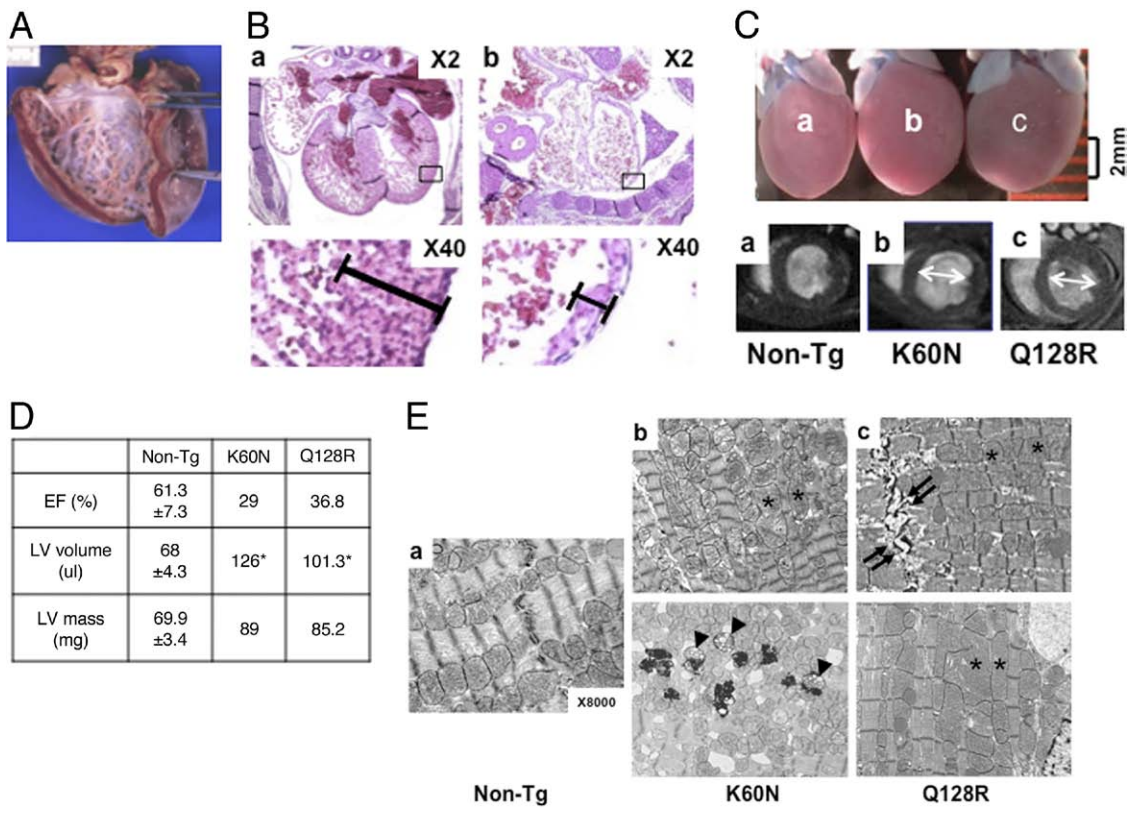

	Non-Tg	K60N	Q128R
EF (%)	61.3 ±7.3	29	36.8
LV volume (ul)	68 ±4.3	126*	101.3*
LV mass (mg)	69.9 ±3.4	89	85.2

Figure 2 **Morphohistologic, Functional, and Ultrastructural Features of Q128R Hearts of Human, Tg Embryos, and Chimeric Mice**

(A) Gross morphology of the Q128R human proband heart (S84-5162). **(B)** Representative hematoxylin and eosin sections of the hearts from **(a)** wild type (WT)-transgenic (Tg) and **(b)** Q128R-Tg embryos at E12.5. **Upper panel** represents ×2 magnification; **lower panel** represents ×40 magnification. **(C)** Representative gross morphology and short-axis left ventricular (LV) end-diastolic cardiac magnetic resonance imaging scans of mouse hearts. Heart enlargement and LV dilation **(arrows)** in K60N-Tg **(b)**, and Q128R-Tg **(c)** chimera mouse hearts compared with non-Tg animals **(a)**. **Bar** = 0.2 cm. **(D)** Cardiac magnetic resonance imaging analysis of mouse hearts (*$p < 0.05$). **(E)** Transmission electron microscopy of WT-Tg **(a)**, K60N **(b)**, and Q128R-Tg **(c)** mouse hearts (×8,000 magnification). **Double arrows** = intercalated disk disruption; **arrowheads** = abnormal lysosomes and mitochondrial remnants; and **asterisks** = enlarged and deformed mitochondria.

osin, cardiac troponin I, cardiac troponin T, and filamin C (Santa Cruz Biotechnology, Santa Cruz, California) were used as recommended by the manufacturers. Multiple sections from at least 5 mice per group were analyzed. Protein expression was quantified using Western blotting, and relative intensity (RI) was carried out using a Kodak Image system (Kodak, Rochester, New York). Beta-actin was chosen as a control, since nebulette only interacts with the muscle elements (α- and F-actin) and not the nonmuscle elements (β-actin) in cardiac background (16).

Nebulette expression in H9C2 cells and differentiation under cyclic mechanical stretch. Rat H9C2 cardiomyoblasts were used to study the effects of nebulette mutations on myofibrillar assembly during differentiation under mechanical stress. Human WT and mutant nebulette cDNA was ligated into a pcDNA3.1NT-GFP-TOPO vector (Invitrogen, Carlsbad, California) and transfected into H9C2 cells plated on BioFlex plates using Effectine (Qiagen, Valencia, California). After 48 h, cells were cultured in Dulbecco's Modified Eagle Medium containing 2% of heat-inactivated horse serum, and subjected to 10% 1-h per day cyclic mechanical stretch for 3 days, as previously described (17). The H9C2 cells were fixed, then stained with anti-GFP and Alexa Fluor Phalloidin-594 (Invitrogen, Carlsbad, California), and visualized using an Olympus confocal microscope (Olympus, San Jose, California).

Statistical analysis. Statistical analysis was performed using Student *t* test and analysis of variance with post-hoc Tukey testing. Data were reported as the mean with standard error of the mean (SEM). Values of $p < 0.05$ were considered significant.

Results

Mutations and clinical correlation. We identified 4 variants in *NEBL*: c.180G>C (exon 3; p.K60N), c.383A>G (exon 5; p.Q128R), c.604G>A (exon 7; p.G202R), and c.1775C>A (exon 17; p.A592E) (Fig. 1A). Variant K60N has previously been reported in the dbSNP database (rs41277374), but neither the population frequency nor the effect on function has been previously reported. Variants K60N, Q128R, and G202R are located in the nebulin-repeat domain, which binds F-actin and tropomyosin-troponin complex, whereas A592E is located in the Z-disk binding region. None of these variants was identified in 300 race- and ethnicity- matched control subjects (600 alleles).

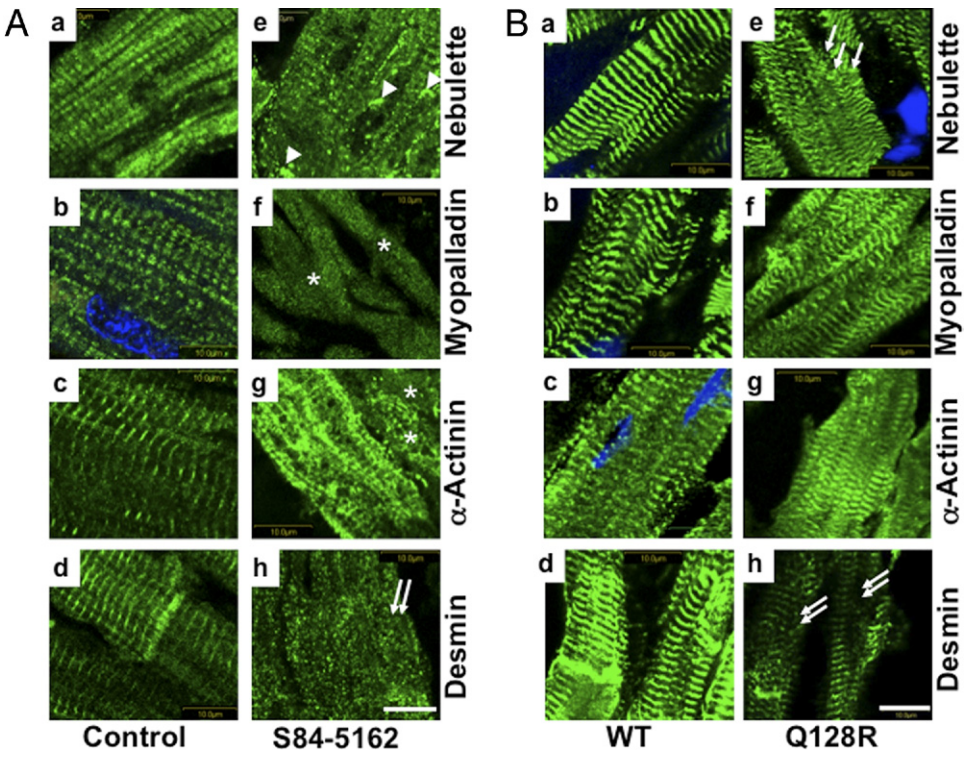

Figure 3 Comparative Immunohistochemical Analysis of Human and Mouse Hearts

(a–d) Sections from **(A)** human and **(B)** WT Tg mouse control hearts. **(e–h)** Sections from the S84-5162 heart **(A)** and Q128R-Tg chimera heart **(B)**, respectively. Nebulette **(a, e)**, myopalladin **(b, f)**, α-actinin2 **(c, g)**, and desmin **(d, h)** are shown in **green**; nuclei are **blue** (4′-6-diamidino-2-phenylindole [DAPI] stain). **Bar** = 10 mm. **Arrowheads** = protein aggregates; **arrows** = diffuse nebulette expression; **asterisks** = smeared protein expression; and **double arrows** = loss of protein. Abbreviations as in Figure 2.

Family analysis was available only for K60N variant, which confirmed the de novo origin of the variant.

The clinical features of the affected subjects hosting these variants were heterogeneous (Fig. 1B). The newborn patient (S84-5162) carrying the Q128R variant had DCM and EFE with a clinical phenotype demonstrating endocardial thickening, deposition of elastic tissue and collagen (Fig. 2A), along with a severely dilated left ventricle and severely depressed systolic function by echocardiography, with a fractional shortening of 10% (Fig. 1B). The child underwent heart transplantation at 8 months of age. The K60N and G202R variants, however, were identified in patients who had clinical manifestations of DCM in adulthood. The patient carrying the A592E variant displayed the clinical features of DCM as a newborn; this patient also carried a digenic mutation in *ACTN2* (Fig. 1B).

Mutations K60N and Q128 cause embryonic lethality and DCM in chimeric mice. Transgenic mouse lines expressing either WT or mutant nebulette under the control of the α-MyHC promoter were made to assess the impact of the NEBL mutations in vivo. The WT, G202R, and A592E mice showed 45%, 40%, and 35% transmission frequencies, respectively. We were unable to identify positive live offspring from K60N and Q128R founders, however. No mutant embryos were harvested from the K60N line at E7.5 or later, whereas mutant Q128R embryos were harvested up to age E12.5. Since K60N Tg embryos numbers were 50% to 70% less than expected, the possibility of embryonic lethality at an earlier stage of development could not be excluded. Histology of the Q128R embryonic hearts revealed severe cardiac changes, including biventricular dilation (Fig. 2B, b; ×2 magnification) and wall thinning (×40 magnification). Such cardiac structural changes are considered to be potential causes of embryonic death.

Founders of the K60N and Q128R lines died at 1 year of age with severe enlargement of the heart (Fig. 2C) and heart failure. Cardiac magnetic resonance imaging of chimeric mice revealed remarkable dilation ($p < 0.05$) (Fig. 2D) compared with control mice. Transmission electron microscopy of hearts revealed enlarged and deformed mitochondria (Fig. 2E, asterisks), abnormal lysosomes, and mitochondrial remnants (Fig. 2E, arrowheads). Localized intercalated disk disruption and accumulation of lipids in cardiomyocytes were noted in Q128R (Fig. 2E, arrows).

Comparative immunohistochemistry of human (control and S84-5162) and transgenic mouse hearts (non-Tg and Q128R) revealed that nebulette was partially disassociated with Z-lines, probably depositing as aggregates throughout the sarcoplasm in the S84-5162 heart (Fig. 3A, e, arrowheads); the Q128R mutant exhibited punctate foci and more diffuse fluorescence for nebulette than the controls (Fig. 3B, e, arrows). Myopalladin (Fig. 3B, f) and α-actinin2 (Fig. 3B, g) were smeared in S84-5162 (Fig. 3B, asterisks), whereas loss of desmin association with Z-disks in both S84-5162 and Q128R-Tg hearts was notable (Fig. 3B, h, double arrows). In Q128R-Tg hearts, myopalladin (Fig. 3B, f) and α-actinin2 (Fig. 3B, g) were not altered.

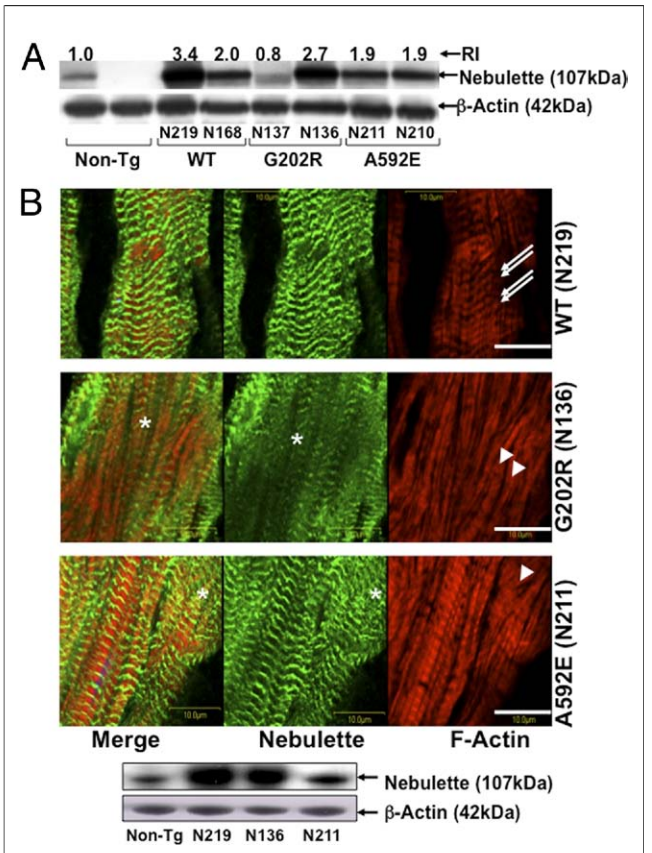

Figure 4 Nebulette Expression in Mouse Hearts

(A) Western blotting of nebulette in mouse hearts. Loading control is β-actin. **(B)** Immunohistochemistry and Western blotting of representative cardiac sections for nebulette **(green)**, F-actin **(red)**, and 4′-6-diamidino-2-phenylindole (DAPI) stain **(blue)**. **Bar** = 10 μm. **Double arrows** = striated F-actin expression; **arrowheads** = diffuse F-actin expression; and **asterisks** = disarray of nebulette. Abbreviations as in Figure 2.

Transgenic G202R and A592E mice exhibit signs of DCM. The WT, G202R, and A592E Tg mice were born and initially developed normally. Protein analysis (Fig. 4A) revealed overexpressed nebulette in N219-WT-Tg, N136-G202R-Tg, and N211-A592E-Tg mouse hearts (RI = 3.4 to 1.9) compared with non-Tg animals (RI = 1.0). This was considered as evidence of overexpressed transgene, and these lines were then bred for further study. Disorganization and disarray of overexpressed nebulette (Fig. 4B, asterisks) along with diffuse expression patterns in F-actin staining in G202R-Tg and A592E-Tg hearts (arrowheads) were detected by immunochemical analysis, compared with WT-Tg hearts (double arrows).

By 6 months of age (Fig. 5A), markedly reduced ($p < 0.01$) tolerance against acute stress, as evidenced by decreased running distances, was observed in G202R mice (270.7 ± 89.0 m) and A592E mice (273.4 ± 55.77 m). On echocardiography (Fig. 5A, lower panels), decreased frac-

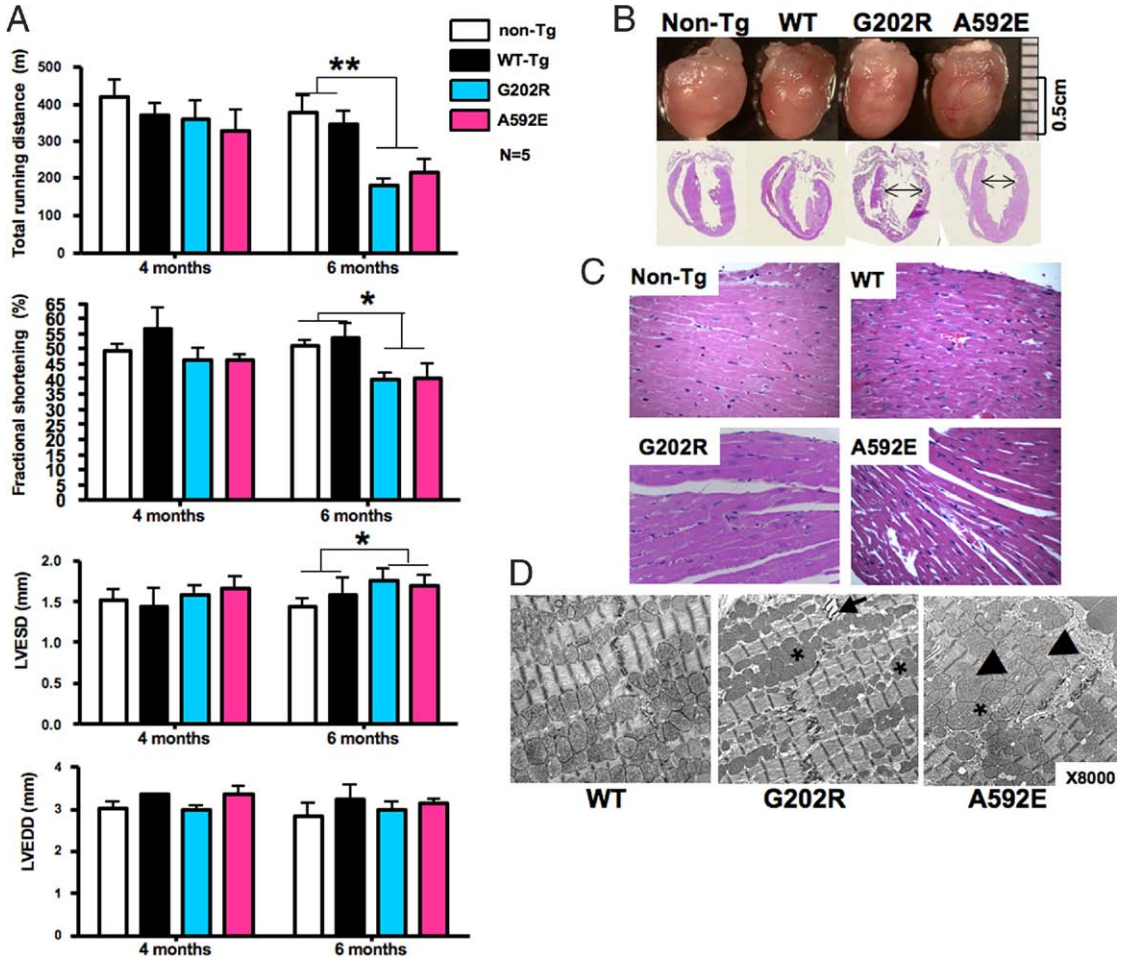

Figure 5 **Cardiac Function and Morphology in Transgenic Mice**

(A) Graded treadmill testing and echocardiography in 4- and 6-month-old mice (n = 5). Mutant G202R mice **(blue bars)** and A592E mice **(pink bars)** exhibited marked reduction in exercise tolerance (**p < 0.01) compared with non-Tg mice **(white bars)** and WT-Tg mice **(black bars)**. Decrease of fractional shortening (*p < 0.05) and increase of left ventricular end-systolic dimension (*p < 0.05) was evident in mutants. **(B)** Morphology and long-axis 4-chamber images of mouse hearts. **Bar** = 0.5 cm. **(C)** Cardiac histology (hematoxylin and eosin, ×40 magnification). Representative sections from non-Tg, WT-Tg, G202R, and A592E are shown. **(D)** Transmission electron microscopy of mouse hearts at ×8,000 magnification. **Asterisks** = enlarged mitochondria; **arrow** = focal separation of intercalated disks; and **arrowheads** = accumulation of lipids and enlarged mitochondria. Abbreviations as in Figure 2.

tional shortening was noted in mutant mice: 50.37 ± 0.7% and 55.24 ± 1.5% in non-Tg and WT-Tg mice, respectively, versus 43.36 ± 3.1% in G202R-Tg mice and 43.14 ± 3.1% in A592E-Tg mice ($p < 0.05$). Significant dilation of the left ventricle was notable, with increased LV end-systolic dimensions in G202R-Tg mice (1.66 ± 0.04 mm) and A592E-Tg mice (1.67 ± 0.02 mm) compared with non-Tg mice (1.47 ± 0.04 mm) and WT-Tg mice (1.51 ± 0.07 mm). No changes in LV end-diastolic dimensions and LV mass-body weight ratio were detected (data not shown).

Cardiac enlargement due to LV dilation (Fig. 5B, arrows), myocyte disarray, and interstitial cell infiltration was evident in G202R and A592E hearts (Fig. 5C). Transmission electron microscopy revealed focal separation of intercalated disks (Fig. 5D, arrow), increased residual body liposome, and mild variation in mitochondrial shape in the G202R mutants (asterisks), whereas the A592E-Tg hearts had mild accumulation of lipids (arrowheads) and abnormalities of mitochondrial shape and size.

Effects of nebulette mutations on I-band and Z-disk composition. Proteins expressed mainly in the I-band, such as cardiac troponin I (RI = 0.5), cardiac troponin T (RI = 0.3), and tropomyosin (RI = 0.2) were significantly down-regulated (Fig. 6B, arrows) and disrupted in G202R-Tg mutants (Fig. 6A, i to l, asterisks). The mobility of filamin C was abnormal in Western blotting, suggesting cleavage (Fig. 6B, arrowhead). In contrast, Z-disk-associated proteins, such as α-actinin-associated LIM protein (RI = 0.2), ZASP (RI = 0.7), α-actinin2 (RI = 0.4), and myopalladin (RI = 0.3) appeared to be down-regulated (Fig. 7B, arrows) and more disrupted (Fig. 7A, m–p, asterisks) in the A592E-Tg hearts. Myopalladin localization

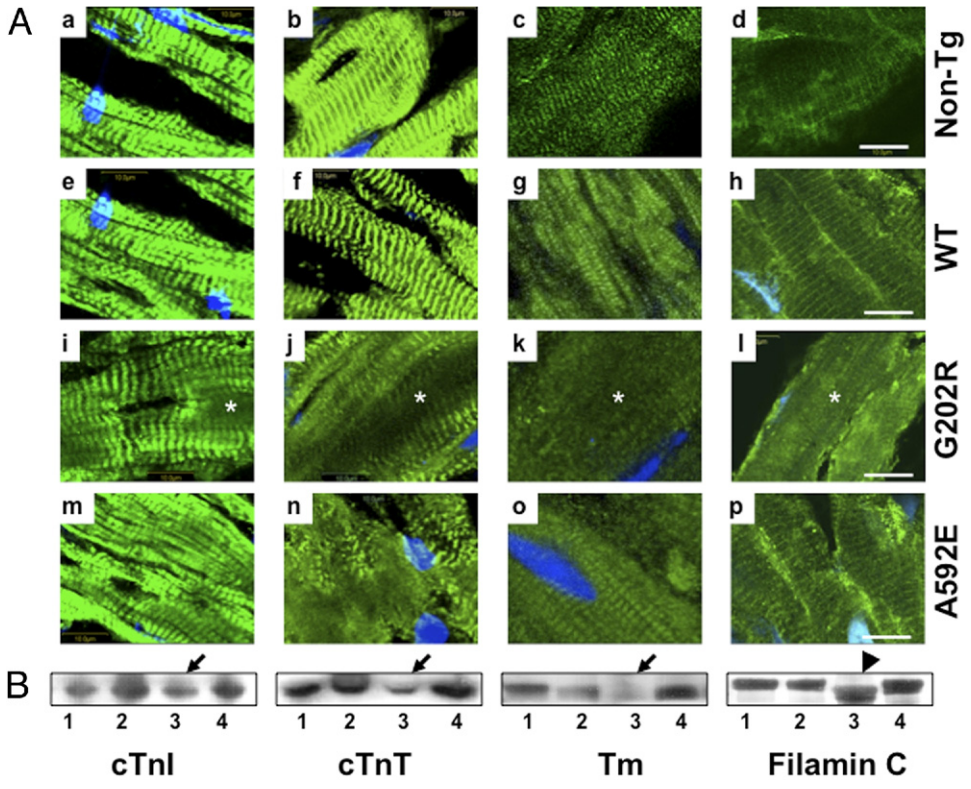

Figure 6 **Comparative Analysis of I-Band Proteins in Mouse Hearts**

(A) Representative cardiac sections stained for cardiac troponin I (cTnI **[a, e, i, and m]**), cardiac troponin T (cTnT **[b, f, j, and n]**), tropomyosin (Tm **[c, g, k, and o]**), and filamin C **(d, h, l, and p)** from non-Tg mice **(a to d)**, WT mice **(e to h)**, G202R mice **(i to l)**, and A592E mice **(m to p)**. Proteins are **green** and nuclei are **blue** (4′-6-diamidino-2-phenylindole [DAPI] stain). **Bar** = 10 mm. **Asterisks** = disrupted expression of proteins. **(B)** Western blotting of I-band proteins in non-Tg hearts **(1)**, WT-Tg hearts **(2)**, G202R-Tg hearts **(3)**, and A592E-Tg hearts **(4)**. Beta-actin is a loading control (Fig. 4B). **Arrows** = down-regulation, and **arrowhead** = cleavage. Abbreviations as in Figure 2.

in Z-disks in G202R-Tg and A592E-Tg hearts appeared normal; however, Western blotting revealed a second lower band in the G202R mice, suggesting cleavage (Fig. 7B, double arrows). Interestingly, α-actinin-associated LIM protein expression was down-regulated in WT hearts (RI = 0.2, arrowhead) compared with non-Tg hearts (RI = 1.0) and G202R-Tg hearts.

Abnormal distribution of mutated nebulette under cyclic mechanical stretch. As a model broadly used in mechanical stretch experiments, rat H9C2 embryonic cardiomyoblasts (ATCC, Manassas, Virginia) was chosen to study the nebulette expression pattern during differentiation. Transfection efficiency of WT- and mutant-nebulette-GFP in H9C2 cells was approximately 10%. Perinuclear cytoplasmic localization of nebulette-GFP was observed in differentiating WT and mutant cells (data not shown).

We hypothesized that nebulette acts as a stretch-induced mechanosensor in cardiomyoblasts (16). To test this, as well as to investigate expression of mutated nebulette in differentiating cardiomyoblasts during mechanical stretch, we performed cyclic mechanical strain of H9C2 cardiomyoblasts. On day 1 of cyclic mechanical stretch, both WT and mutant nebulette-GFP were localized uniformly (Fig. 8A, d, g, and j; higher resolution, inset) to the perinuclear region in differentiating cells (asterisks). By day 3, WT nebulette-GFP was distributed throughout the cytoplasm along with F-actin filaments reaching the periphery of cells (Fig. 8B, d to f, arrows) and tended to form lines, presumably assembling into the maturating Z-lines (higher resolution, right corner). In contrast, despite being normally extended to the periphery of the sarcoplasm F-actin filaments (Fig. 8B, g to l, arrowheads), sustained perinuclear nebulette-GFP localization in all mutants was evident (asterisks; Q128R and A592E mutants representing I-band and Z-disk mutations, respectively, are shown).

Discussion

Over the past decade, variants in a many genes encoding structural proteins have been reported in patients with cardiomyopathies (1). In particular, genes encoding cytoskeletal and sarcomeric proteins, including Z-disk proteins, have been found to be the "final common pathway" of DCM (18). The events leading to EFE are not well

JACC Vol. 56, No. 18, 2010
October 26, 2010:1493–502

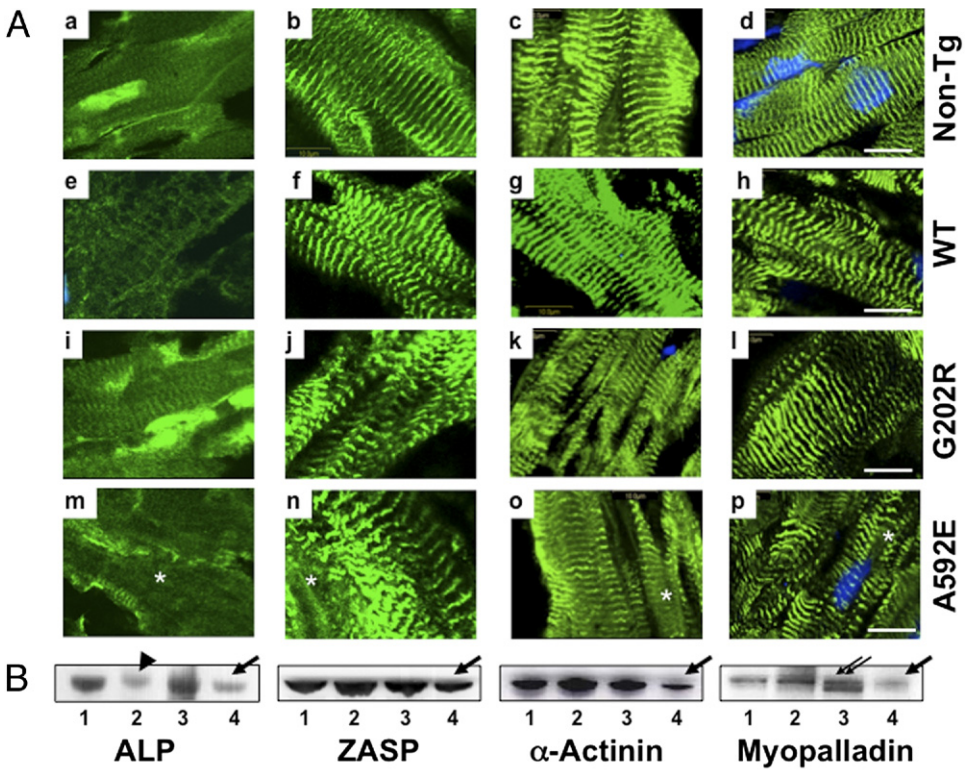

Figure 7 **Comparative Analysis of Z-Disk Proteins in Mouse Hearts**

(A) Representative cardiac sections stained for α-actinin-associated LIM protein (ALP **[a, e, i, m]**), ZASP **(b, f, j, n)**, α-actinin2 **(c, g, k, o)**, and myopalladin **(d, h, l, p)** from non-Tg mice **(a to d)**, WT mice **(e to h)**, G202R mice **(i to l)**, and A592E mice **(m to p)**. Proteins are **green**, and nuclei are **blue** (4′-6-diamidino-2-phenylindole [DAPI] stain). **Bar** = 10 mm. **Asterisks** = disrupted expression of proteins. **(B)** Western blotting of Z-disk proteins in non-Tg mouse hearts **(1)**, WT mouse hearts **(2)**, G202R mouse hearts **(3),** and A592E mouse hearts **(4)**. Beta-actin is a loading control (Fig. 4B). **Arrows** and **arrowhead** = down-regulation, **double arrows** = cleavage.

understood, but have been reported to result from an environmental insult, including virus or chemical exposure, in a genetically susceptible person (2,3). The goal of this study was to uncover the molecular basis of cardiac dysfunction in subjects with DCM, focusing on genes encoding proteins of the sarcomere and Z-disk. Four *NEBL* gene variants (K60N, Q128R, G202R, and A592E) were identified in patients with DCM and EFE. We demonstrated that these mutations lead to a variety of cardiac phenotypes and levels of severity in vivo, from embryonic lethality due to a severe cardiac abnormalities (K60N and Q128R), to postnatal DCM with clinical signs of impairment in cardiac function (G202R and A592E) as seen in humans recapitulating the human disease phenotype, with or without EFE. Interestingly, G202R and A592E mutations were found to result in cardiac dysfunction despite causing different ultrastructural changes. The I-band proteins were significantly disrupted in G202R mouse hearts, whereas the Z-disk associated proteins appeared to be more disrupted in the A592E hearts. These findings led us to hypothesize that *NEBL* mutations have different effects on protein function depending on the location of the mutation in specific portions of the nebulin repeats.

Nebulette is a component of the early dense body structures involved in myofibrillogenesis of developing cardiac muscle (8,9). We demonstrated that cyclic mechanical strain is a factor that initiates the distribution of nebulette to the sarcomere, being an important determinant in stimulating formation of Z-lines in differentiating H9C2 cardiomyoblasts. To support this hypothesis, we evaluated *NEBL* mutations to determine whether the mutations affect nebulette distribution and differentiation in cardiomyoblasts, and found no abnormalities occurred. When H9C2 cells were subjected to cyclic strain, however, we demonstrated that *NEBL* mutations perturbed the codistribution of nebulette-GFP throughout the sarcomere with the actin filaments and delayed expression of nebulette-GFP in the maturing Z-lines.

Taken together, these data support our hypothesis that nebulette functions as a mechanosensor and may have signaling properties in stretch-induced activation of specific mechanotransduction pathways in cardiomyoblasts during myogenesis. These data also support our in vivo results that demonstrate that expression of mutant Q128R nebulette leads to severe structural abnormalities in the embryonic heart, and thus, ultimately to embryonic lethality. More-

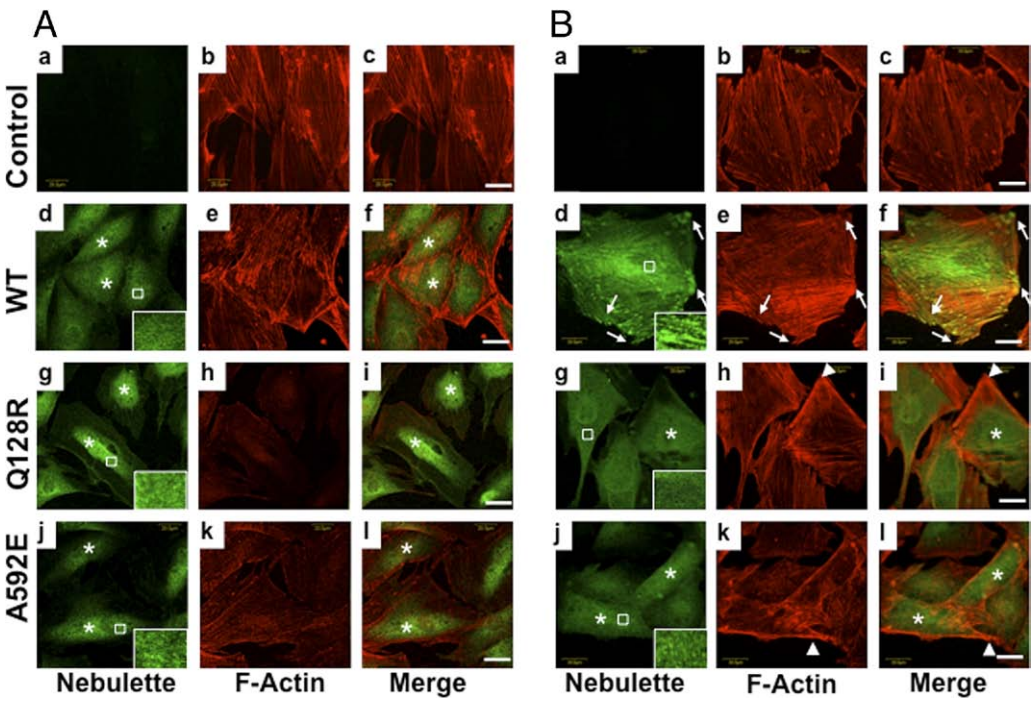

Figure 8 **Cyclic Mechanical Stretch of H9C2 Cells**

(A) Day 1. **Asterisks** = uniformly expressed nebulette. **(B)** Day 3 of cyclic strain. Control rat H9C2 cardiomyoblasts are shown **(a to c)**. Nebulette **(green, left panels)**, actin **(red, middle panels)**, and merge images **(right panels)** are shown in H9C2 cells transiently expressing wild-type (WT)- **(d to f)**, Q128R- **(g to i)**, and A592E-nebulette-GFP **(j to l)**. Bar = 20 mm. Experiments were repeated 3 times to confirm stability of results. **Arrows** = expression of F-actin in the maturating Z-lines; **arrowheads** = absence of nebulette in the periphery of the sarcoplasm; and **asterisks** = expression of nebulette in perinuclear region.

over, an abnormal expression pattern for nebulette, myopalladin, and desmin was discovered in the heart of a child carrying the Q128R mutation. It suggests that interruption of these proteins may cause specific EFE phenotype in humans. We speculate that the nebulette-desmin protein-protein interaction transmits information from the Z-disks to the intermediate filaments, maintaining the structural and functional integrity of myocytes (12). On the basis of its timing during embryogenesis, as well as its functional effects on key binding partners, it appears likely that the Q128R mutation alters cardiac development, specifically affecting myofibrillogenesis through the early nebulette-actin interactions and later nebulette-desmin association. We speculate that disruption in nebulette-actin codistribution and/or delay in nebulette expression in the maturating Z-disks at the earliest stages of myogenesis may be present in K60N mice.

In contrast to K60N and Q128R, the fact of down-regulated tropomyosin and troponins in the mutant mice as an effect of G202R mutation suggests that this mutation may cause changes in force generation in mature cardiomyocytes (19). Our data are consistent with the data reported by Bonzo et al. (7) in which overexpression of nebulette fragments was associated with loss of endogenous nebulette, tropomyosin, and troponins accompanied with a decrease in thin filament length and concomitant loss of F-actin. In addition, nebulin repeats were found to contribute to the assembly and the allosteric properties of the striated muscle thin filament (14). Although we did not measure cardiac actin level and actin-filament length in the G202R mice, it is likely that dysregulated tropomyosin, troponins, and filamin C cause the development of LV dilation in our model.

The A592E mutation, in contrast, led to cytoarchitectural changes with different patterns of expression of Z-disk proteins, and dysregulation of Z-disk proteins suggests that A592E may disturb force transmission. Myofibrillar functional integrity is regulated by the Z-disk network linking the sarcomere, cytoskeleton, sarcoplasmic reticulum, and sarcolemma (4). Mature cardiomyocytes respond to mechanical stretch with an immediate increase in contractility as well as long-term changes in gene expression resulting in myocyte hypertrophy (5). Orchestrated cross-talking between multiple independent and mechanosensitive signaling pathways such as MAPK, PI3K/Akt, Ras, JAK/STAT, and Ca^{2+} signaling determines the final phenotype of the cardiomyopathies. The desmin-based unit is one of the major contributors in mechanotransduction (12,16), and it appears that the I-band–nebulette–Z-disk connection may play a crucial role in transmitting information from the Z-disks to the intermediate filaments.

JACC Vol. 56, No. 18, 2010
October 26, 2010:1493–502

Conclusions

In summary, we identified novel nebulette mutations (K60N, Q128R, G202R, and A592E) in patients with DCM, EFE, and cardiac failure. We propose that *NEBL* is a new susceptibility gene for EFE and DCM and that these mutations lead to cardiac remodeling and dysfunction. This work suggests that disruption of the proposed signaling pathways leads to unfavorable cardiac remodeling and, consequently, cardiac dysfunction. Furthermore, mutations in certain domains of nebulette alter the function of its interacting proteins in a distinct, domain-defined manner and ultimately will result in activation and/or disruption of signaling cascades, culminating in structural remodeling of cardiomyocytes.

Reprint requests and correspondence: Dr. Jeffrey A. Towbin, The Heart Institute, Cincinnati Children's Hospital Medical Center, 3333 Burnet Avenue, Cincinnati, Ohio 45229. E-mail: jeffrey.towbin@cchmc.org.

REFERENCES

1. Towbin JA, Lowe AM, Colan SD et al. Incidence, causes, and outcomes of dilated cardiomyopathy in children. JAMA 2006;296:1867–76.
2. Kamisago M, Schmitt JP, McNamara D, et al. Sarcomere protein gene mutations and inherited heart disease: a beta-cardiac myosin heavy chain mutation causing endocardial fibroelastosis and heart failure. Novartis Found Symp 2006;274:176–89, 272–6.
3. Ni J, Bowles NE, Kim YH, et al. Viral infection of the myocardium in endocardial fibroelastosis. Molecular evidence for the role of mumps virus as an etiologic agent. Circulation 1997;95:133–9.
4. Pyle WG, Solaro RJ. At the crossroads of myocardial signaling: the role of Z-discs in intracellular signaling and cardiac function. Circ Res 2004;94:296–305.
5. Towbin JA, Bowles NE. The failing heart. Nature 2002;415:227–33.
6. Bonzo JR, Norris AA, Esham M, Moncman CL. The nebulette repeat domain is necessary for proper maintenance of tropomyosin with the cardiac sarcomere. Exp Cell Res 2008;314:3519–30.
7. Grunewald TG, Butt E. The LIM and SH3 domain protein family: structural proteins or signal transducers or both? Mol Cancer 2008;7:31.
8. Moncman CL, Wang K. Nebulette: a 107 kD nebulin-like protein in cardiac muscle. Cell Motil Cytoskeleton 1995;32:205–25.
9. Esham M, Bryan K, Milnes J, et al. Expression of nebulette during early cardiac development. Cell Motil Cytoskeleton 2007;64:258–73.
10. Bang ML, Mudry RE, McElhinny AS, et al. Myopalladin, a novel 145-kilodalton sarcomeric protein with multiple roles in Z-disc and I-band protein assemblies. J Cell Biol 2001;153:413–27.
11. Wang X, Osinska H, Gerdes AM, Robbins J. Desmin filaments and cardiac disease: establishing causality. J Card Fail 2002;8 Suppl 6:287–92.
12. Holmes WB, Moncman CL. Nebulette interacts with filamin C. Cell Motil Cytoskeleton 2008;65:130–42.
13. Ogut O, Hossain MM, Jin JP. Interactions between nebulin-like motifs and thin filament regulatory proteins. J Biol Chem 2003;278:3089–97.
14. Arimura T, Nakamura T, Hiroi S, et al. Characterization of the human NEBL gene: a polymorphism in an actin-binding motif is associated with nonfamilial idiopathic dilated cardiomyopathy. Hum Genet 2000;107:440–51.
15. Yang Z, Bowles NE, Scherer SE, et al. Desmosomal dysfunction due to mutations in desmoplakin causes arrhythmogenic right ventricular dysplasia/cardiomyopathy. Circ Res 2006;99:646–55.
16. Moncman CL, Wang K. Targeted disruption of nebulette protein expression alters cardiac myofibril assembly and function. Exp Cell Res 2002;273:204–18.
17. Kumar A, Murphy R, Robinson P, Wei L, Boriek AM. Cyclic mechanical strain inhibits skeletal myogenesis through activation of focal adhesion kinase, Rac-1 GTPase, and NF kappaB transcription factor. FASEB J 2004;18:1524–35.
18. Bowles NE, Bowles KR, Towbin JA. The "final common pathway" hypothesis and inherited cardiovascular disease. The role of cytoskeletal proteins in dilated cardiomyopathy. Herz 2000;25:168–75.
19. Lammerding JAN, Kamm RD, Lee RT. Mechanotransduction in cardiac myocytes. Ann NY Acad Sci 2004;1015:53–70.

Key Words: dilated cardiomyopathy ■ endocardial fibroelastosis ■ mutation ■ nebulette.